Edited by J.F. Nie, A.J. Morton and B.C. Muddle

Micro-Mechanistic Crack Closure Modelling of Constant Amplitude and Variable Amplitude Fatigue in Damage Tolerant Airframe Aluminium Alloys

K. H. Khor[1], N. Kamp[1], K. D. Singh[1], M. R. Parry[1, 2], Y. Xu[1, 2], I. Sinclair[1]

[1] Materials Research Group, School of Engineering Sciences, University of Southampton, Southampton, U.K.
[2] Current address: Damage Tolerance Department (ESADU), Airbus, Filton, Bristol, UK.

Keywords: Fatigue, aluminium alloy, crack closure, modelling, constant amplitude, variable amplitude

Abstract

The incidence of crack closure has been widely recognised as a major factor affecting fatigue growth rates via the shielding of cyclic load conditions in the crack-tip region. However, significant problems exist in both the experimental determination and micromechanical modelling of closure behaviour. In the present work, detailed micro-mechanistic models to predict crack closure levels under constant amplitude (CA) and variable amplitude (VA) loading conditions are discussed, considering the influences of plasticity-induced crack closure (PICC) and roughness-induced crack closure (RICC). Results are compared to experimental data for a variety of airframe aluminium alloys.

1. Introduction

In quantifying the fatigue crack growth behaviour of a material, it is possible to identify intrinsic and extrinsic contributions to failure resistance, with intrinsic resistance representing the inherent mechanical and environmental material response to cyclic loading at the crack tip. Extrinsic resistance represents the influence of internal mechanical processes that attenuate, or shield, the cyclic loading actually experienced in the crack tip region. Since the identification of fatigue crack shielding via crack closure (*viz*. mechanical contact of crack surfaces at loads above the applied cyclic load minimum) by Elber [1], it has been widely recognised as a major extrinsic influence on the crack propagation resistance of common structural materials, including airframe aluminium alloys [2]. Several mechanisms of crack closure have been identified, including plastically induced crack closure (PICC), roughness-induced crack closure (RICC) and oxide-induced crack closure (OICC).

For many engineering alloys, the most significant origins of crack closure may be identified as the essentially mechanical process of PICC, and the more microstructurally dependent RICC. PICC is defined as the premature contact between crack faces caused by the residual plastically deformed material left behind a crack during (cyclic) crack advance. Various engineering tools for fatigue life prediction under variable amplitude loading conditions have indeed been developed from detailed treatments of PICC (e.g. the comprehensive work of Newman and co-workers, see [3, 4]). RICC may be particularly identified with the microstructural influences on crack path, and is associated with mismatch between fracture surfaces exhibiting surface asperities behind the crack tip.

Several attempts have been made to model RICC, e.g. see [5, 6]. However, previously available models, to the best of the authors knowledge, all suffer from an essentially arbitrary treatment of the shear offsets required for the asperities in a crack wake to come into physical contact during unloading. RICC influences on variable amplitude fatigue (i.e. representative of service conditions for most engineering components) has also been recognised, particularly in relation to enhanced post-overload fatigue performance in Al-Li alloys [7].

2. CA Crack Growth Analysis

Previous work by Parry and co-workers has identified residual shear deformation in the wake of a deflecting crack as the primary factor in determining RICC, see [8]. This process is illustrated schematically in Figure 1, highlighting the role of irreversible shears at the turning point of a given crack path asperity.

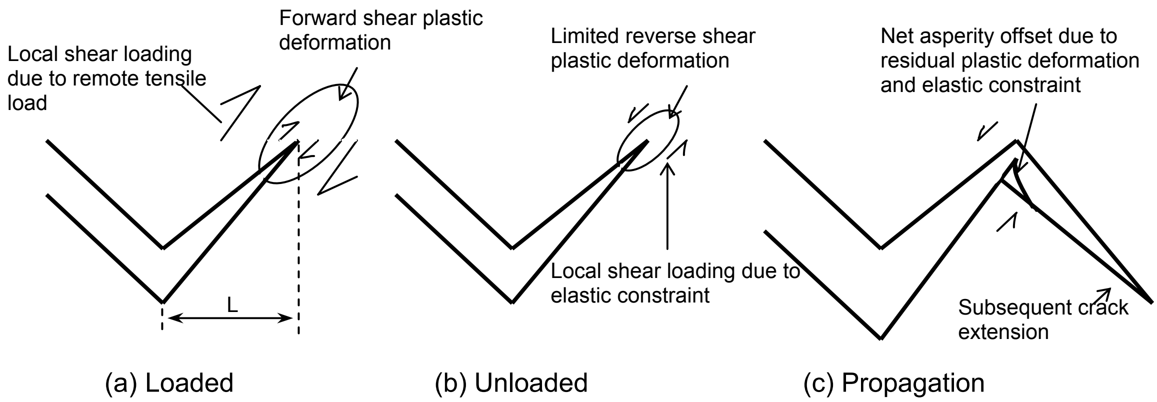

Figure 1: Schematic of RICC arising from residual crack shear at asperities.

Corresponding two-dimensional (2D) analytical modelling [9] has been used to describe the effective mode II residual shear associated with a crack passing through a single representative crack turning point (i.e. asperity tip) and the subsequent fracture surface contact that will arise as the crack tip moves away from this point. The main elements of this model are estimating the crack opening along the deflected crack path as a function of applied load, and the mode II residual shear deformation (characterised by the crack tip sliding displacement) at the crack turning point that will interfere with this opening (i.e. to generate crack closure). Based on this approach, closure levels for a simple zig-zag crack under CA loading and plane strain conditions are given by the following simplified expression,

$$\frac{K_{cl}}{K_{\mathrm{I}max}} = \beta \frac{\sqrt{3\pi} K_{\mathrm{I}max} \left(\frac{1}{2} + R - \frac{1}{2} R^2 \right) \left(\sin\frac{\theta}{2} + \sin\frac{3\theta}{2} \right)^2 \sin 2\theta}{16\sigma_{YS} \sqrt{a^*} \left(3\cos\frac{\theta}{2} + \cos\frac{3\theta}{2} \right)} \tag{1}$$

where K_{cl} is the closure stress intensity, K_{Imax} is the maximum applied mode I stress intensity, σ_{YS} is the yield stress of the material, and β is a scaling factor which may be expected to be between 1 and 4. θ is the nominal crack deflection angle and a^* is the distance of the tip to the previous crack turning point. With Equation (1) being implemented in relation to each crack turning point, it is clear that the model exhibits a singularity, i.e. when a^* tends to zero. This arises from the model neglecting the requirement for deformation to pass into the crack wake to generate closure. As such, a propagation distance that is required for deformation to act fully in the closure process is identified and expressed as some fraction, λ , of the plastic zone size, r_p, with λ then being derived from FE analysis and/or experimental data [9]. It is interesting to note that whilst crack deflection angle has a major effect on closure levels in the above model, an underlying relationship between RICC effects and plastic zone size emerges: specifically, RICC effects decrease rapidly as the asperity size falls below the active plastic zone size. This effect is illustrated in Figure 2 [9] by the predictions of peak RICC levels in a 2024-type material as a function of L/r_p where L is the projected length of a single deflected crack segment in a simple 45˚ zig-zag crack path (see Figure 1). Good correlation between the above analytical modelling and equivalent finite element results is also highlighted.

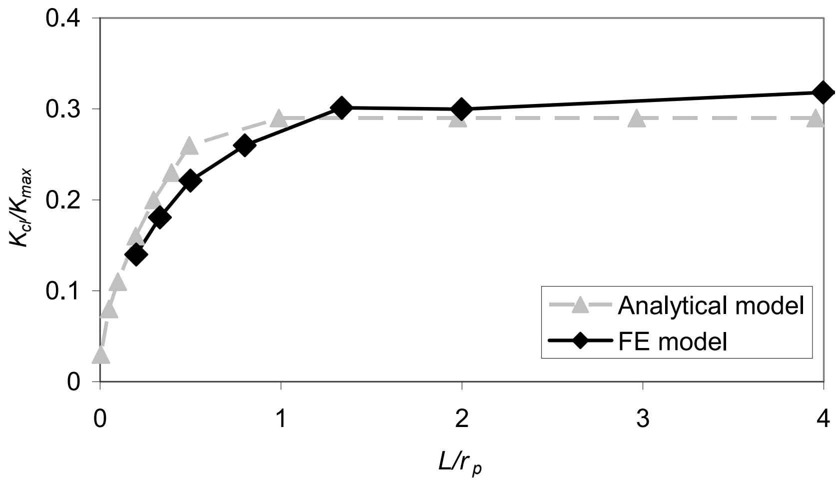

Figure 2: Comparison of analytical and finite element predictions of RICC effects for a simple 45˚ zig-zag crack path in a 2024-T351 type material, as a function of crack deflection length L, normalised by plastic zone size, r_p.

Comparisons between measured and modeled crack closure levels for a variety of 2xxx-type alloys under plane strain conditions are illustrated in Figure 3 and Figure 4. Results in Figure 3 are derived from six different several dilute Al-Cu-Mg-(Li) alloys discussed elsewhere in these proceedings [10]. Predicted closure levels were based on Talysurf measurements of the corresponding fracture surfaces (i.e. identifying representative θ and L values [11]), with a representative fracture area being measured for each alloy in the low ΔK regime where RICC effects may be expected to be most significant. Whilst an ideal one-to-one prediction of closure levels is not achieved in this case (closure predictions tend to be low), the trend in closure levels between the various alloys is reasonably well predicted. Figure 4 considers three microstructural conditions of the advanced damage tolerant alloy, 2027-T351 (a high dispersoid variant of 2024), with closure predictions being made from Talysurf measurements at two stress intensity levels for each material. It may be seen that predicted closure levels again tend to be low, however the increase in closure levels with decreasing stress intensities is well represented, as indeed is the similarity in closure levels between the three materials. Overall it may be seen that whilst exact closure levels are under predicted to some extent, similarities and difference between alloys are reasonably well capture by the modelling.

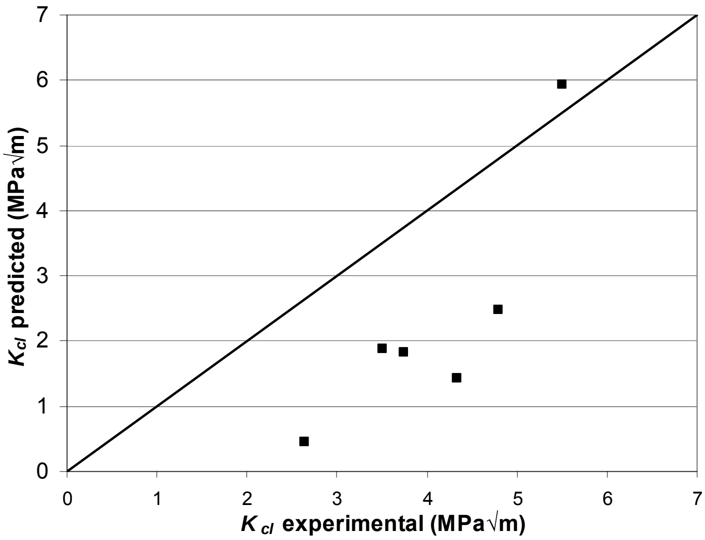

Figure 3: Correlation of measured and predicted crack closure levels measured at low stress intensity levels (ΔK between 3 and 7 MPa√m) for a range of Al-Cu-Mg-(Li) alloys.

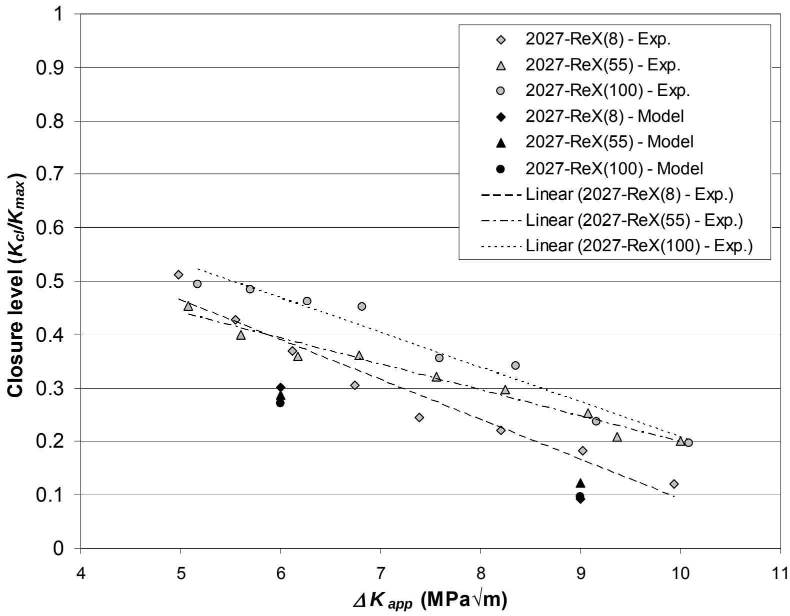

Figure 4: Comparison of experimentally measured closure levels (as a function of applied stress intensity range) and analytical model predictions for 8%, 55% and 100% recrystallised 2027-T351 plates (designated ReX(8), ReX(55) and ReX(100) respectively)

3. VA Crack Growth Analysis

In the first instance a simple modification of the above model may be made for single overload growth conditions by letting shear displacement at the deflection point be defined by the overload transient conditions. Crack opening displacements beyond the deflection point are then assumed to be governed by baseline loading, and treated elastically as before. Whilst this approach cannot treat the evolution of near-threshold growth modes that often occurs after overloads, it should still provide an indication of RICC contributions to the early peak in closure levels.

Following this approach, the closure level for an overloaded deflected crack can be expressed as;

$$\frac{K_{cl}}{K_{\mathrm{I}\max}} = \beta \frac{\sqrt{3\pi} K_{\mathrm{I}\max}\left(\xi + R - \frac{1}{2}R^2 - \frac{1}{2}\right)\left(\sin\frac{\theta}{2} + \sin\frac{3\theta}{2}\right)^2 \sin 2\theta}{16\sigma_{YS}\sqrt{a^*}\left(3\cos\frac{\theta}{2} + \cos\frac{3\theta}{2}\right)} \tag{2}$$

Where ξ is the ratio of the overload and baseline maximum stress intensities. In keeping with Equation (1), the model exhibits a singularity (when a^* tends to zero), with the propagation distance needed for deformation to act in the closure process again be identified as a fraction, λ , of the overload plastic zone size, r_{pOL}.

As noted earlier, RICC effects are predicted to decrease dramatically when the asperity size falls below the active plastic zone size. With overload plastic zone sizes of necessity being larger than the associated baseline loading (plastic zone size scales with the square of the stress intensity), an important prediction of this model is that that relatively large asperity sizes are needed for effective RICC contribution to overload transients. In the case of an overloaded crack, two conditions of closure effect may then be considered to arise: (1) when crack asperity sizes are small relative to overload plastic zone size, tensile displacements associated with the load transient are most effective in generating closure and the overload transient is essentially a PICC controlled event and microstructural effects are limited, and (2) when crack asperity sizes are large relative to overload plastic zone size, shear displacements associated with the load transient are more effective in generating closure and the overload transient is enhanced by RICC effects. The present models predict that for typical Paris regime growth conditions (ΔK of the order of 10MPa√m, R = 0.1 for example), in a moderate strength airframe alloy (of the order of 400MPa), crack path asperity dimensions (i.e. L) of 500μm are required for a full RICC contribution to a 100% overload transient, i.e. a relatively large scale compared to fracture surface features seen in conventional airframe alloys [12]. This is consistent with experimental plane strain overload results shown in Figure 5 [13], showing essentially similar overload transient effects in 2024 and 2024A-T351 materials, even though increased baseline/CA crack growth resistance of the 2024A was clearly linked to increased fracture surface roughness and RICC effects [14]. The results of Vankateswara Rao and Ritchie [7] are then of some interest in providing a direct comparison of the Al-Li alloy 2090-T8E41 with a 2124-T351 alloy. Large crystallographic facets are particularly evident on fracture surfaces of the 2090-T8E41 material, with individual major crack deflections being seen to occur for distances of the order of hundreds of micrometres. Figure 6 shows a comparison of plane strain overload transient responses for the 2124 and 2090 material, with the 2090 results clearly showing the stronger overload transient. For the load conditions associated with Figure 3 and the associated tensile properties of the materials [7], fracture surface asperity sizes of the order of 250μm are predicted to be sufficient for a strong RICC contribution in the Al-Li alloy, consistent with the scale of surface features seen in this material and its significantly increased overload transient effect.

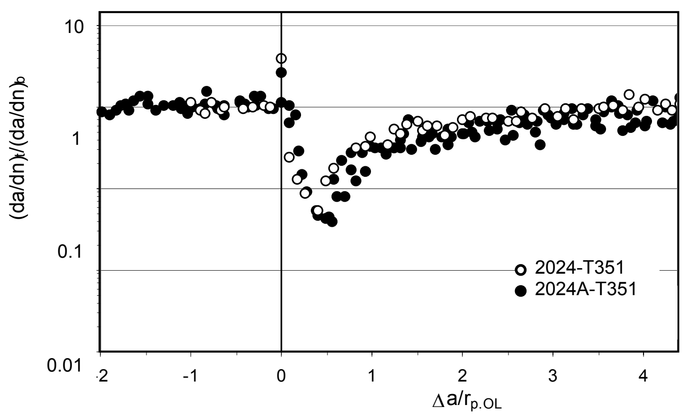

Figure 5: Normalised crack growth rate transients following a single 100% overload cycle in 2024 and 2024A-T351 at a baseline stress intensity range of 12MP√m, R = 0.1. Transient growth rates ($(da/dn)_t$) are normalised in terms of the baseline growth rate ($(da/dn)_b$) for the relevant alloy. Δa represents the distance of the crack tip from the overload location.

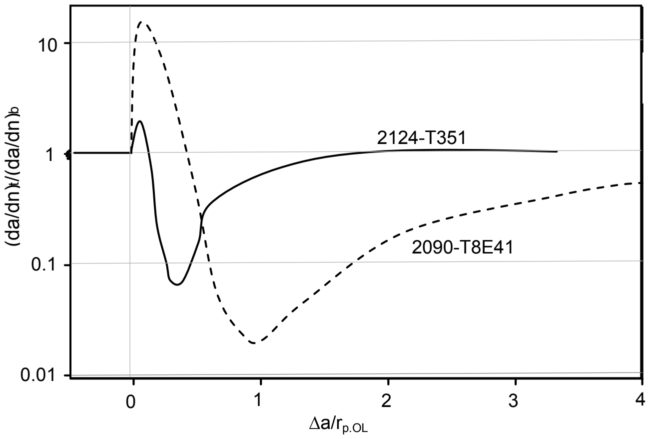

Figure 6: Normalised crack growth rate transients following a single 150% overload cycle in 2090-T8E41 and 2124-T351 at a baseline stress intensity range of 8MP√m, R = 0.1. Transient growth rates ($(da/dn)_t$) are normalised in terms of the baseline growth rate ($(da/dn)_b$) for the relevant alloy. Δa represents the distance of the crack tip from the overload location [7].

4. Summary and Conclusions

Physical interpretation of RICC effects in terms of residual shear displacements at crack wake asperities has been modelled, with predictions being compared to a variety of experimental (and finite element) results. For constant amplitude loading conditions, where the model is most readily applied, predictions of plane strain crack closure levels from real fracture surface features has been shown to be in reasonable functional accord with experimental data. The model is readily extended to single overload growth conditions, at least in terms of estimating the scale of fracture surface features needed to produce significant RICC effects during an overload transient. Such predictions are seen to be in good accord with transient behaviour seen in conventional and Al-Li-based alloys.

Acknowledgements

The authors wish to acknowledge Pechiney CRV (France) for funding and materials supply.

References

[1] W. Elber, Engineering Fracture Mechanics, 1970. 2: p. 37-45.

[2] J.C. Newman and W. Elber, Mechanics of Fatigue Crack Closure, ASTM STP 982.

[3] J.C. Newman, FASTRAN-II - A fatigue crack growth structural analysis program, NASA Technical Memorandum 104159. 1992.

[4] J.C. Newman, Analyses of fatigue crack growth and closure near threshold conditions for large-crack behaviour, NASA Technical Memorandum 209133. 1999.

[5] S. Suresh and R.O. Ritchie, Metallurgical Transactions, 1982. 13A: p. 1627-1631.

[6] J. Llorca, Fatigue & Fracture of Engineering Materials & Structures, 1992. 15: p. 655.

[7] K.T.V. Rao and R.O. Ritchie, Acta Metallurgica, 1988. 36: p. 2849-2862.

[8] M.R. Parry, S. Syngellakis, and I. Sinclair, Materials Science and Engineering A, 2000. 291: p. 224-234.

[9] N. Kamp, M.R. Parry, K.D. Singh, and I. Sinclair, Acta Materialia (in press), 2003.

[10] N. Kamp, M.J. Starink, N. Gao, I. Sinclair, P.J. Gregson, P.D. Pitcher, and S. Gardiner, these proceeding, 2004.

[11] N. Kamp, N. Gao, M.R. Parry, and I. Sinclair, Metallurgical Transactions (in press), 2003.

[12] K.D. Singh, Modelling of combined roughness and plasticity induced closure effects in high strength Al-alloys. MPhil/PhD Transfer Thesis, University of Southampton. 2003.

[13] Y. Xu, Closure assessment and overload transient behaviour in damage tolerant airframe materials. Ph.D thesis, University of Southampton. 2001.

[14] Y. Xu, P.J. Gregson, and I. Sinclair, Materials Science Forum, 2000. 331: p. 1525-1530.